International Journal for Multidisciplinary Research (IJFMR)
E-ISSN: 2582-2160 ● Website: www.ijfmr.com ● Email: editor@ijfmr.com

Investigating Damage in Reinforced Concrete Members by Using Vibrating Wire Strain Gauge

Hussain Ahmed Sheikh[1], Sadam Hussain[2], Asad Nadeem[3], Muhammad Usman[4], Muhammad Usman Hanif[5]

[1,2,3,4]Student, Civil Engineering, National University of Sciences and Technology (NUST), Pakistan
[5]Assistant Professor, Civil Engineering, National University of Sciences and Technology (NUST), Pakistan

Abstract:
Recently the use of vibrating wire strain gauges has increased to find out the damage in a reinforced concrete structure. The assembly and functioning of this acoustic strain gauge are presented. This gauge provides numerous benefits including its sensitivity to measure strain (up to 1micron) and its property of being easily attached on any concrete surface. The gauge apparatus can be made in a lab due to its low cost which gives it an edge over the conventional systems. The gauge was calibrated after considering the variations in temperature.
The purpose of the experimentation was to set up a low-cost vibrating wire strain gauge, calibrate it and use it for static strain damage assessment of a reinforced concrete beam. The strain readings from the vibrating wire strain gauge were cross-checked using a Demec gauge. Discrete Fourier transforms moving window was utilised to analyse the vibration signals specifically the change in natural frequency with respect to time. The gauge setup provided a cheap and accurate way for measuring long-term static strain in reinforced concrete structures. The results are presented and reviewed.

Keywords: Strain Gauge, Damage Assessment, Natural Frequency, Fourier Transformation, Vibration Signals, Temperature Variations

1. Introduction:

Researchers have been interested in the monitoring/damage assessment of the reinforced concrete structures at early structures, such as (Chakraborty et al., 2019) and (Ai et al., 2023). Traditional methods revolve either around detecting cracks visually or using localized experimental methods such as ultrasonic and acoustic techniques like (Kozlov et al., 1997). The requirement of these methods is that the precise location of the cracks is recognized and approachable. Therefore, recent methods primarily focus on the changes that take place in the vibrational properties of the structure itself., as work done by the (Nigam & Singh, 2020) and (Mishra et al., 2019). However, the existing work that has been done using the vibrational techniques conformed with the assumption that the vibrations are linear (Mousavi et al., 2021). Which meant that the modal properties of the structure did not change with the amplitude of the oscillations.
This involves the need of the measurement of strain in order of tens of $\mu\varepsilon$ to a higher degree of accuracy. The standard electrical resistance gauges are unable to measure at such degrees of accuracy. Moreover, these gauges are not suitable when it comes to attaching them on the concrete surface as they are unable

to bridge the cracks. Hence, the vibrating wire strain gauge proves to be a useful alternative. These gauges in comparison to the traditional gauges provide us with strains of accuracy in the order of hundreds of micro strain (Neild et al., 2005). Other advantages of the vibrating wire strain gauge include the easiness of attachment and its ability to take measurements with cracks on the specimen.

The vibrating wire strain gauge consists of a pre-tensioned steel wire between two fixed supports attached on the specimen to be assessed. When there is a change in the property of the concrete specimen it brings upon a change in the tension of the wire, resulting in the variation in fundamental frequency. This variation is then to be related to the value of deformation with the help of physical-mathematical models.

One of the limitations of the use of a vibrating wire strain gauge is its sensitivity to the variations in temperature. 1˚ change in temperature results in a 20 $\mu\boldsymbol{\varepsilon}$ change in the strain of the wire(Neild et al., 2005). This error is linked with the differences between the thermal expansion coefficients of both the gauge and the concrete specimen.

The vibrating wire strain gauge was developed with the aim of attaching it to the concrete surface and using it for measuring strains in the specimen.

2. Literature Review:

2.1 Frequency Strain Relationship:

If a wire is held rigidly at both ends the expression for its fundamental frequency can be derived using the principle of stationary waves discussed above

$$v = \sqrt{\frac{Fxl}{m}}$$

$$v = \sqrt{\frac{F}{m/l}}$$

Dividing up and down by Area A

$$v = \sqrt{\frac{F/A}{m/V}}$$

$$v = \sqrt{\frac{\sigma}{\rho}}$$

Here

- A = Area of wire
- V = Volume of wire
- ρ = density of the wire
- σ = Stress the wire

As we know the relationship between frequency and speed for the first mode of vibration is

$$f_1 = \frac{v}{2l}$$

$$f_1 = \frac{1}{2l}\sqrt{\frac{\sigma}{\rho}}$$

For the nth mode of vibration as for example (Parker, 1997)

$$f_n = \frac{n}{2l}\sqrt{\frac{\sigma}{\rho}}$$

2.2 Strain in Specimen:

For a specimen shown in the figure below:

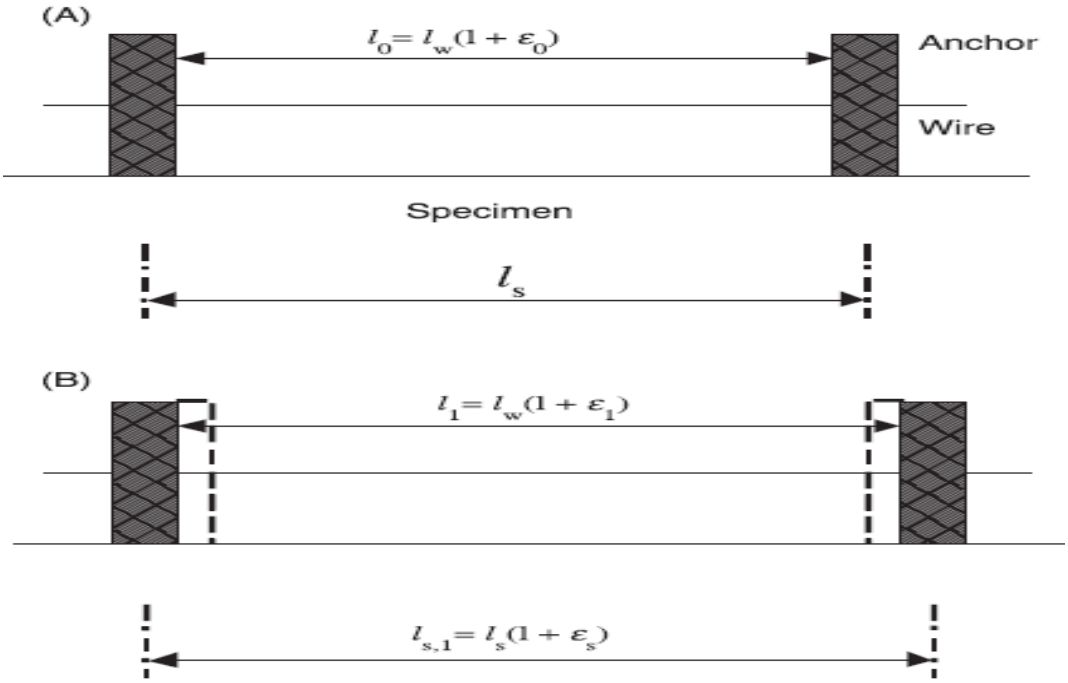

Figure 1: Strained and Unstrained specimen

- Lw =Unstretched length
- l0 = total span held at tension
- E = Modulus of Elasticity

The strain in the specimen can be calculated by (Parker, 1997) :

$$f_o = \frac{1}{2l_o}\sqrt{\frac{E\epsilon_o}{\rho}}$$

Where,

$$\epsilon_o = \frac{l_o - l_w}{l_w}$$

After loading

$$\epsilon_1 = \frac{l_1 - l_w}{l_w}$$

And its natural frequency will be

$$f_1 = \frac{1}{2l}\sqrt{\frac{E\varepsilon_1}{\rho}}$$

Strain in the specimen is

$$\varepsilon_s = \frac{l_{s1} - l_s}{l_s} = \frac{l_1 - l_o}{l_s}$$

The ratio of frequencies before loading and after loading is

$$\frac{f}{f_o} = \frac{l_o}{l}\sqrt{\frac{\epsilon}{\epsilon_o}}$$

Using above expressions

$$\frac{f}{f_O} = \frac{1}{1+\frac{l_s}{l_o}\epsilon_o}\sqrt{1+\frac{l_s}{l_w}\frac{\epsilon_s}{\epsilon_o}} \cong \sqrt{1+\frac{l_s}{l_w}\frac{\epsilon_s}{\epsilon_o}}$$

Considering the strain in the specimen is very small, $\frac{1}{1+\frac{l_s}{l_o}\epsilon_s}$ is equal to unity. So,

$$\frac{f_1}{f_o} = \frac{l_o}{l_o + l_s\varepsilon_s}\sqrt{1+\frac{l_s\varepsilon_s}{l_w\varepsilon_o}}$$

Rearranging

$$\epsilon_s = \frac{l_o\epsilon_o}{l_s fo^2}(f^2 - fo^2) = G(f^2 - fo^2)$$

Where G is the gauge factor. Its value only depends on the material of the wire and is independent of the initial strain in the wire or specimen. The value of the gauge factor can be determined theoretically by

$$G = \frac{l_o\epsilon_o}{l_s fo^2} = \frac{4lo^3\rho}{l_s E}$$

Normally, the value of the gauge factor is calculated through experimental calibration which will be explained in the coming sections.

2.3 Effect of Temperature:

Suppose we have temperature variation between the two frequency readings. If the coefficients of thermal expansion of wire and specimen are the same there will be no change in the strain as both specimen and wire will expand with the same factor. On the other hand, if coefficients of thermal expansion of wire and specimen are different then the effect of temperature on strain becomes significant. An additional strain will generate due to temperature. It is mandatory to have two gauges, one is for the loading test and the other is for the measurement of relative change in strain due to temperature. Both gauges should be in an identical operating environment. So total strain due to load and temperature can be measured by

$$\epsilon_s = \epsilon_{load} + (T - T_O)(\alpha_m - \alpha_w) = G(f^2 - fo^2)$$

Introducing,

$$F = (f^2 - fo^2)$$
$$\epsilon_s = \epsilon_{load} + (T - T_O)(\alpha_m - \alpha_w) = GF$$

Where

- T0 = Initial Temperature
- T1 = Final Temperature
- F = Difference of the squares of the frequencies
- α_s = Expansion coefficients of specimen
- α_w = Expansion coefficients of wire

To eradicate this temperature, we use a control gauge which is held close to the specimen or sample. So above equation will become.

$$\varepsilon_s{}^{load} = G({f_1}^2 - {f_0}^2 - {f_{c1}}^2 + {f_{c0}}^2)$$

Where

- f_{co} = frequency of control gauge at T0
- f_{c1} = frequency of control gauge at T1
- f_0 = frequency of loading gauge before straining
- f_1 = frequency of loading gauge after straining

3. Methodology

The basic process of developing the gauge and using it for damage assessment can be broadly divided into 4 categories:

1) Experimental setup of the gauge
2) Calibration of the gauge
3) Test Setup and Loading Regime
4) Signal Processing

3.1 Experimental Setup of the Gauge

The assembly of the vibrating wire strain gauge is quite simple. For the gauge, two M8 bolts were glued onto the concrete surface with the help of epoxy. The center-to-center distance between the two bolts was kept 100 mm corresponding to the crack spacing occurring at the stirrup locations. A hole was drilled next to the bolt head to allow the wire to pass through. A guitar string having a diameter of 0.1" was passed through the bolts and was pre-tensioned to a force of 14.72 N with the help of a spring balance. The wire was clamped by the use of well lubricated washers and by tightening the nut. This allowed for the wire to be held in place at the initial tension. The figure below shows the setup of the gauge as viewed from the top and the side.

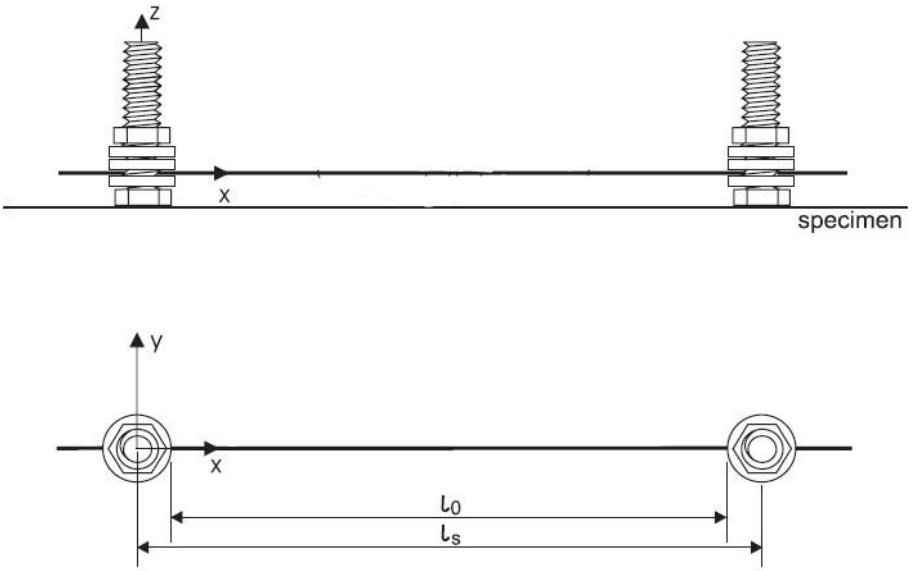

Figure 2: Gauge Setup Model

As for recording the vibrating wire audio signal, a microphone was clamped onto the bolts near to the string. A low pass filter of 2500 Hz was applied, and the sampling frequency was fixed at 8 KHz. The microphone was then connected to a computer and then the audio was recorded and edited using a Digital

Audio Workstation. The wire was excited 5 times in succession and then the frequency of each signal was averaged to find out the frequency of the signal. The variation in the frequency content for each strain condition did not deviate by more than ± 0.15%. During this procedure of acquiring the signal, the unstrained control gauge was kept close to the test sample to minimize the effect of temperature on the frequency content of the signal.

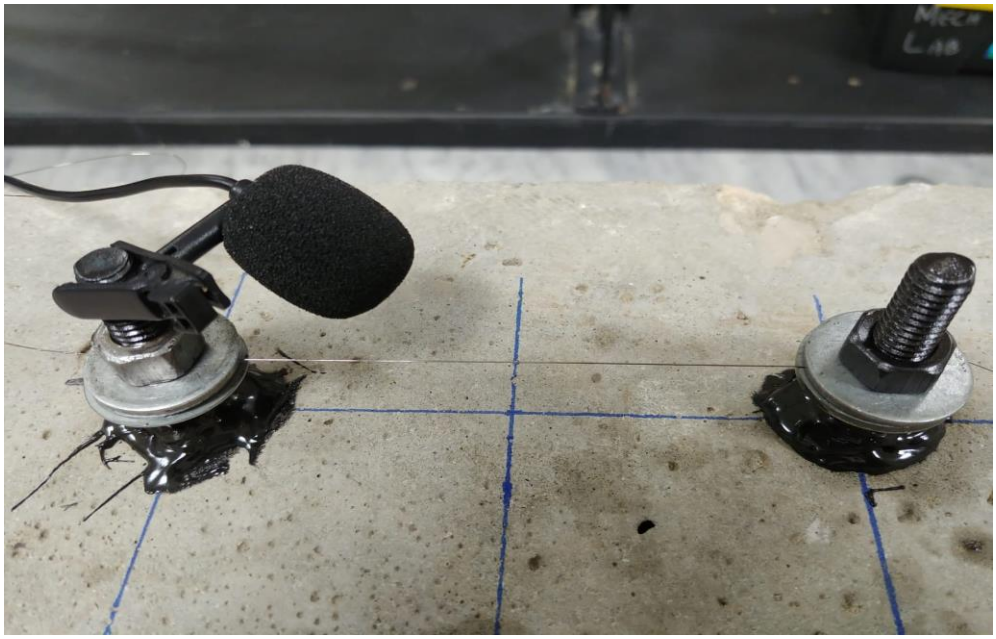

Figure 3: Gauge Setup Practical

3.2 Calibration of the Gauge

For both the strained and unstrained circumstances, the specimen strain was computed using the reference and measurement gauge frequencies. These frequencies may be combined using equation 6.14 to compute the strain in terms of the gauge factor, G, in comparison to the unstrained state.

Figure 4: Calibration Gauge Setup on Nylon Bar

To calibrate the gauge, tests were conducted on a bar of nylon having cross-sectional dimensions of 16 mm x 16 mm and a length of 300 mm. The Young's Modulus of nylon is 2.7 GPa. Hooks were inserted into the rod at each end and the rod was hanged at one end to allow no moment transfer at the supports. Known loads were applied at the other end by hanging them with the hooks.

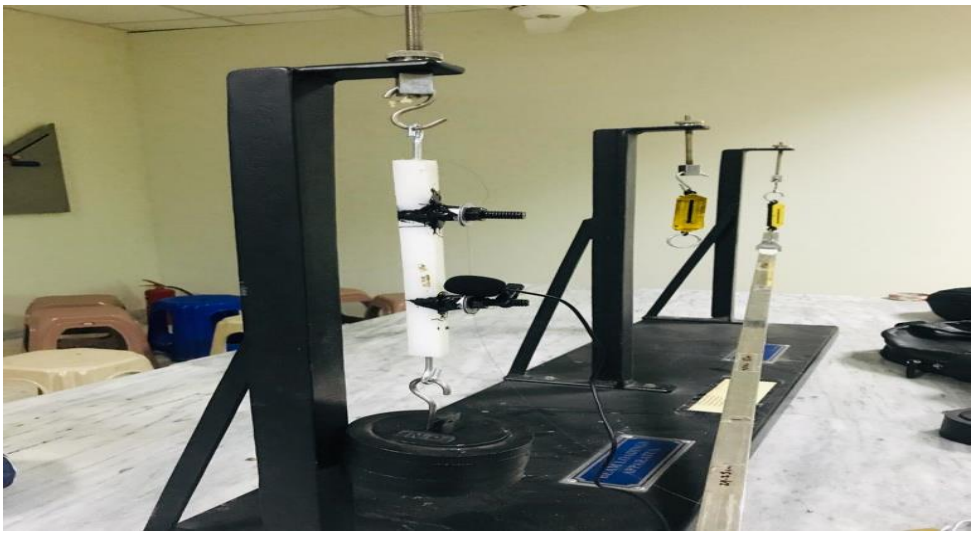

Figure 5:Loading Applied on Nylon Bar to Induce Applied Strain

An increment of 5N was applied in each test and the corresponding frequency of the signal was obtained using the same procedure as mentioned above. The change in frequency with incremental load was then determined and a relationship was developed between the factor F (difference in the square of frequencies at strained and unstrained level) and the applied load.

3.3 Test Setup and Loading Regime

Static strain tests were conducted on the reinforced concrete beams and the strain readings from the vibrating wire strain gauge and Demec gauge were compared to cross-validate the accuracy of the strain gauge. The beams were loaded using the 4-point bend test to investigate the effect of pure flexure on the beam. 3 identical reinforced concrete beams having a cross-section of 100 mm x 150 mm x 1500 mm were casted using the same mix design. The main reinforcement were 9.525 mm bars having a yield strength of 413.69 MPa. The stirrups were 6.35 mm bars of 413.69 MPa yield strength being placed at a center-to-center distance of 100 mm.

Figure 6: Beam Placed on Loading Rig to Induce Damage

Vibrating wire strain gauges were attached at midspan to the beam surface at depths of 25 mm and 125 mm from the top of the beam. Demec pips were glued onto the concrete surface on the opposite face of the beam at the same depths corresponding to the location of the vibrating wire gauges. This ensured that both the Demec gauge and the vibrating wire strain gauge measured the same strain along the cross-section thereby allowing validation of the strain measurements made from the vibrating wire strain gauge.

Figure 7: Strain Measurements Using Demec Gauge

The beam was loaded incrementally in a loading rig and the extent and location of cracks were studied. The load was applied in increments of 500 kg till the failure of the beam. Simultaneous readings of strain were taken from both the demec and vibrating wire strain gauges at each damage level.

Figure 8:Cracking Induced in Beam due to Loading

3.4 Signal Processing

The frequency content of the recorded signal was processed and analysed. The signal comprised of two closely spaced peaks in the frequency domain. A potential reason for this could be because of the difference in stiffness offered by the supports in the y and z directions. The wire was vibrated from the centre in the z-direction but some vibration in the y-direction was inevitable. The figure below shows a typical time-domain signal recorded from the vibrating wire strain gauge.

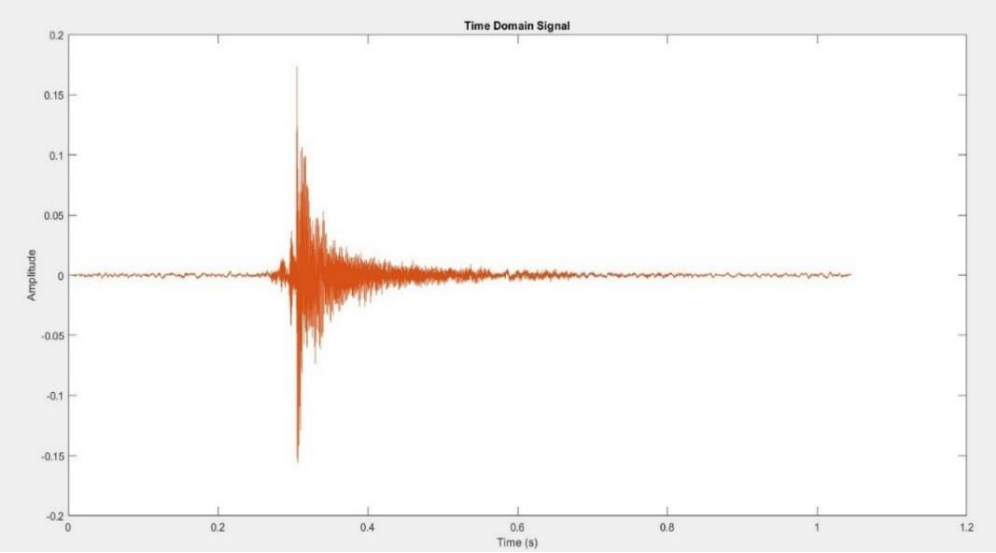

Figure 9: A Typical Time Domain Signal

To determine the frequency content of the signal, the Fast Fourier Transform (FFT) of the signal was performed. The highest frequency peak of the signal corresponded to the frequency of the wire. The figure below shows a typical FFT graph of a signal acquired from the vibrating wire strain gauge. The initial peak has the highest amplitude but is discarded as it corresponds to the background noise. Next, the highest peak in the frequency domain plot is taken as the natural frequency of the wire which in this case turned out to be 902.68 Hz. This frequency for the unstrained gauge could be cross-checked by the theoretical value of frequency for the gauge using the mathematical equation described above. The graph below shows a particular frequency domain plot of the signal.

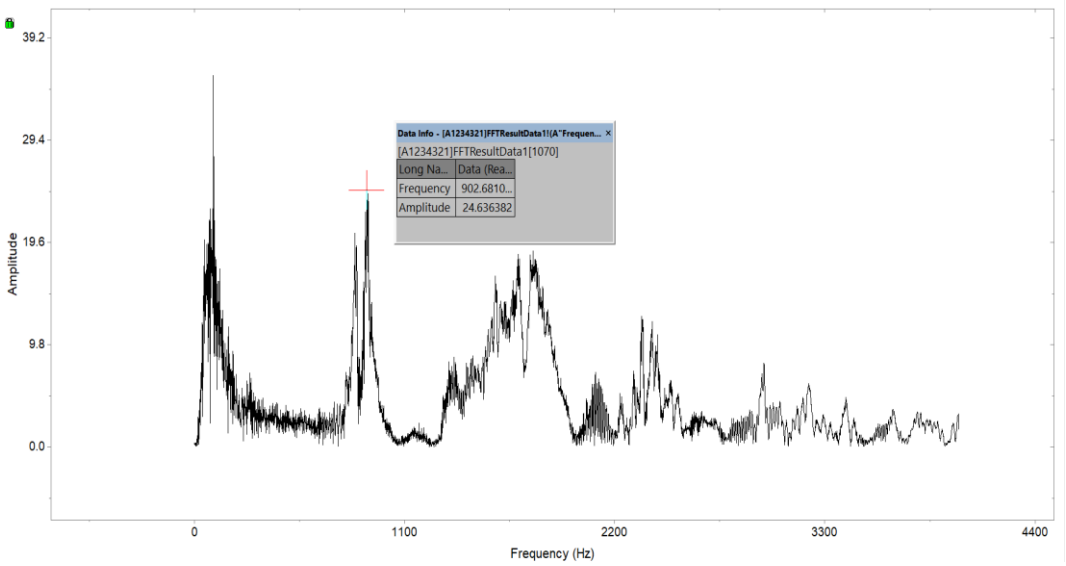

Figure 10:Typical Frequency Domain Plot of Signal

However, since the initial signal is non-linear, it is essential that the non-linear portion of the signal be removed. This was done by determining the time-frequency relationship of the signal. The time-frequency relationship provides information regarding the constituent frequencies that the signal is composed of at a particular time instant. This relationship was determined by the Short-Time Fourier Transform (STFT) of the signal. For the STFT, the Hanning window function having an FFT length of 512 bins and an overlap

of 256 bins was selected. Once the time-frequency relationship was obtained, the time till which the signal remains non-linear is removed from the signal and the FFT of the remaining signal is performed for the next 1.5 seconds. After 1.5 seconds the signal-to-noise ratio decreases substantially and so the frequency content cannot be determined accurately (Neild, 2005). The figure below shows an STFT graph obtained from the strain gauge signal.

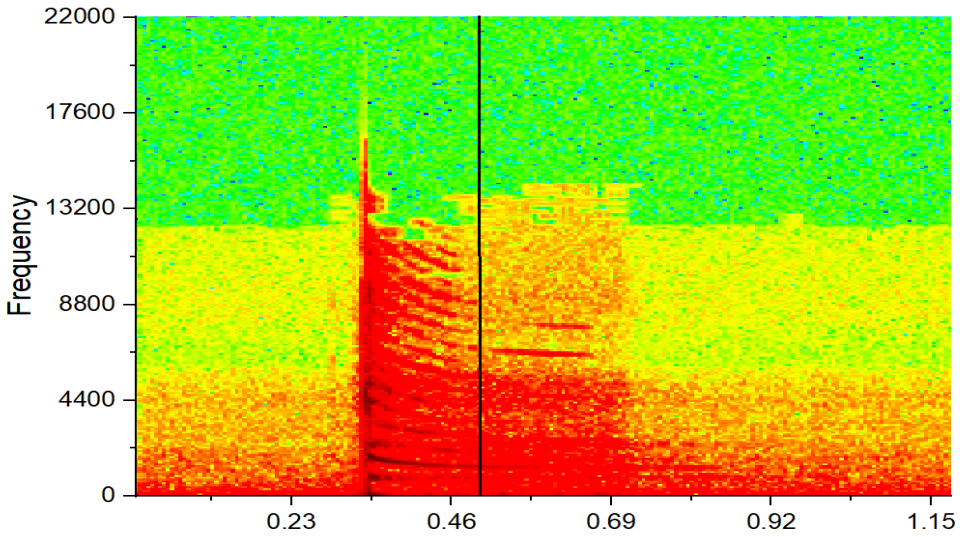

Figure 11:A Typical Frequency-Time Plot of the Signal

It is evident from the graph that the wire is excited at 0.345s and begins to exhibit linear behavior after 0.49s. The amplitude corresponding to the time at which the signal begins to exhibit linear behavior is then identified as the threshold amplitude. The threshold amplitude for each gauge was determined and was kept the same for each loading condition. Once the amplitude of the signal falls below the threshold amplitude, the FFT of the next 0.5 seconds of the signal is done to obtain its frequency content. To filter the signal, a band pass filter having a bandwidth of 300 Hz was applied centered at the natural frequency of the wire to remove additional noise from the signal. The figure below shows the difference between the time domain plot of the filtered and unfiltered signal.

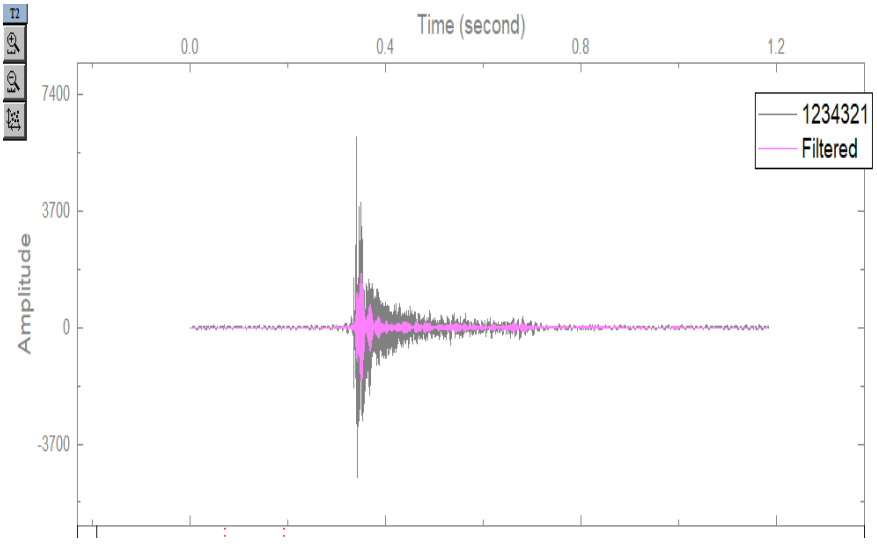

Figure 12:Time Domain Plot of Filtered and Unfiltered Signal

4. Results and Discussion

4.1 Gauge Calibration Results

For the calibration of the gauge, different readings were taken at different levels of applied strains. The readings are presented below in the tabulated form.

Gauge Calibration				
Load	**Stress**	**Strain**	**Frequency**	**F**
0	0.0	0.0	955	0.0
10	39062.5	14.5	980.8	49943.6
20	78125.0	28.9	1051.1	192786.2
30	117187.5	43.4	1123.6	350452.0
40	156250.0	57.9	1183.2	487913.6
50	195312.5	72.3	1229.7	600137.1
60	234375	86.8	1290.9	754397.8

Table 1: Gauge Calibration Data

From these readings, a graph between the factor F and the applied strain was plotted. The Gauge Factor G is obtained by determining the gradient of the line of best fit between the two variables. The multiplication of the gauge factor with F for any damage level gives us the strain at that damage level.

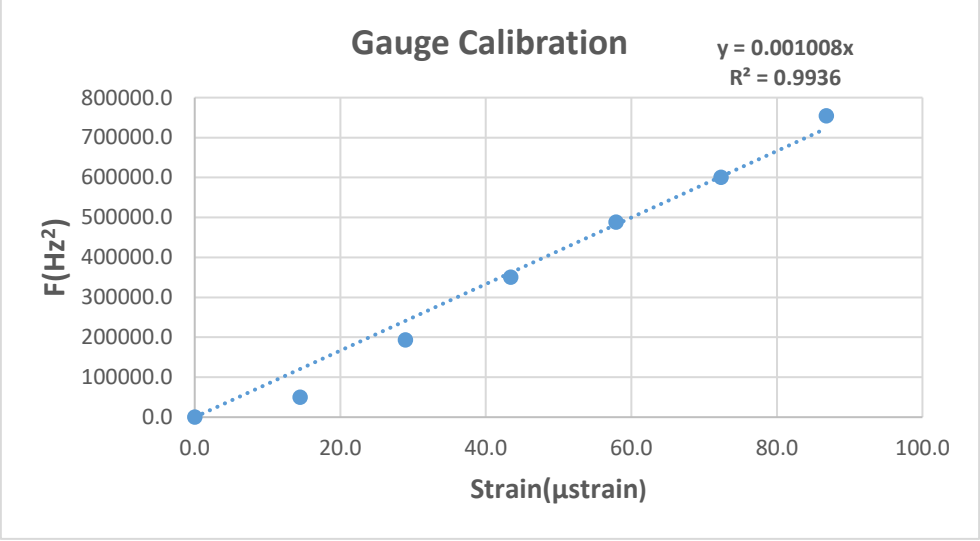

Figure 13: Gauge Calibration Graph

The graph above shows the relationship between F and applied strain. The gauge factor G was determined to be 1.008 x 10^{-9}. The coefficient of determination turned out to be 0.9936. An important point to note here is that the relationship between F and applied strain is linear.

4.2 Strain Response

The cross-validation of the strain gauge readings with Demec gauge readings was done by 4-point loading on beams. Throughout the testing, the control gauge was placed in the same environment as that of the

test beams to minimize temperature differences. The fluctuation in temperatures was not so great so as to affect the readings of both the gauges. The table below shows the values obtained from the Demec gauge and the vibrating wire strain gauge.

Beam Test					
Load (kg)	**DG**	**Frequency (Hz)**	**Strain(μstrain)**	**Difference**	**Error (%)**
0	0	902.69	0	0	0
500	640	1197.7	624.6	15.4	2.41
1000	1210	1409.2	1180.4	29.6	2.45
1500	1986	1647	1912.9	73.1	3.68
1794		failure load			

Table 2: Demec Gauge and Vibration Wire Strain Gage Comparison

Prior to reaching the 2500 kg damage level, the cracking of the beam caused the gauge to detach from the concrete surface because of which the vibrating wire strain gauge reading was not determined. The average error in the readings was 4.62%. This goes to show that the vibrating wire strain gauge has the ability to accurately measure static strains in structures.

5. Conclusion and Future Recommendations

The use of vibrating wire strain gauge provides a cheap and reliable method for long term damage assessment of structures like bridges, water towers etc. The design and setup of a vibrating wire strain gauge is presented. The vibrating wire strain gauge presented has the capability to measures strain accurately and so can be used for strain measurement purposes in structures.

To further strengthen the design of the gauge proposed, the future work should be aimed at automating the process of signal acquisition and processing which would allow the acquisition of live strain data. This would be particularly useful as it would reduce the tedious task of repeatedly acquiring and processing the signal and would also give strain readings for the present time thereby improving the health monitoring procedure. Another recommendation would be to incorporate a thermistor in the current design of the gauge to remove the need of presence of control gauge near to the test gauge to remove the temperature effects.

6. References

1. Ai, D., Jiang, G., Lam, S.-K., He, P., & Li, C. (2023). Computer vision framework for crack detection of civil infrastructure—A review. *Engineering Applications of Artificial Intelligence*, *117*, 105478.
2. Chakraborty, J., Katunin, A., Klikowicz, P., & Salamak, M. (2019). Early Crack Detection of Reinforced Concrete Structure Using Embedded Sensors. *Sensors*, *19*(18), 3879. https://www.mdpi.com/1424-8220/19/18/3879
3. Kozlov, V., Samokrutov, A., & Shevaldykin, V. (1997). Thickness measurements and flaw detection in concrete using ultrasonic echo method. *Nondestructive Testing and Evaluation*, *13*(2), 73-84.

4. Mishra, M., Barman, S. K., Maity, D., & Maiti, D. K. (2019). Ant lion optimisation algorithm for structural damage detection using vibration data. *Journal of Civil Structural Health Monitoring*, *9*, 117-136.
5. Mousavi, M., Holloway, D., Olivier, J., & Gandomi, A. H. (2021). Beam damage detection using synchronisation of peaks in instantaneous frequency and amplitude of vibration data. *Measurement*, *168*, 108297.
6. Neild, S. A., Williams, M. S., & McFadden, P. D. (2005). Development of a Vibrating Wire Strain Gauge for Measuring Small Strains in Concrete Beams. *Strain*, *41*(1), 3-9. https://doi.org/https://doi.org/10.1111/j.1475-1305.2004.00163.x
7. Nigam, R., & Singh, S. K. (2020). Crack detection in a beam using wavelet transform and photographic measurements. Structures,
8. Parker, M. N. a. P. (1997). *Advanced Level Physics,* . Heinemann Educational.